Polish J. Chem., **78**, 1509–1521 (2004)

Electrooxidation of *o*-Aminobenzylalcohol – Identification of Oligo-benzylether Structures and Polyaniline Type Polymer by IR and UV/VIS Spectra[*]

by B. Boczek and B. Palys[**]

Laboratory of Electrochemistry, Department of Chemistry, University of Warsaw,
Pasteura 1, 02-093 Warsaw, Poland

(Received March 11th, 2004; revised manuscript May 6th, 2004)

The electrooxidation of *o*-aminobenzylalcohol was studied in aqueous acidic solutions. Two distinct electroactive and electrochromic products were identified by cyclic voltammetry, *in situ* UV/VIS and infrared spectra. In initial electrodeposition cycles the oligomers containing benzylether units are formed. Further oxidation–reduction cycles lead to the polyaniline-type polymer. Effects of the kind of acid present in the polymerization bath and of the acid concentration were also studied.

Key words: poly (*o*-aminobenzylalcohol), electropolymerization, anion effect, FTIR, benzylether

Substituted polyaniline (PANI) derivatives have been studied extensively in order to influence the optical properties, to enhance the solubility in organic solvents or to enhance the polymer usefulness in metal cation binding [1–6]. Conductivity of substituted derivatives is often lower comparing to PANI, although methoxy-substituted polyanilines are good conductors and additionally they are soluble in common organic solvents [7–10]. Aniline derivatives with hydroxy or second amine groups in the *ortho* position polymerize giving oxazine or phenazine linkages between the benzene units. Such conjugated ladder type polymers are characterized by a single redox couple and different electronic absorption spectra comparing to PANI [11–16].

It has been reported that the isomer compound of *o*-aminobenzylalcohol (ABA) – *o*-methoxyaniline also yields the polymer, having the electrochemical properties similar to PANI together with the dimer containing oxazine ring as the by-product [17,18].

This paper reports the electrochemical and spectroscopic studies on ABA electrooxidation. It is shown that two distinct electroactive and electrochromic species are formed during the ABA electrooxidation. The electrooxidation products are investigated by cyclic voltammetry, *in situ* UV/VIS and infrared spectra. The influence of

---

[*] Dedicated to Prof. Dr. Z. Galus on the occasion of his 70th birthday.

[**] Corresponding author; e-mail: bpalys@chem.uw.edu.pl

the kind of acid and of the acid concentration on poly-*o*-aminobenzylalcohol (PABA) formation is demonstrated.

EXPERIMENTAL

The electrooxidation was carried out in the solution containing 0.1 M ABA. The acid concentration was equal to 0.2, 1.0 or 2.0 M of H_2SO_4 and 0.4, 2 or 4 M of $HClO_4$. The electrochemical experiments were performed in a single compartment cell with a conventional three electrode configuration using silver-silver chloride electrode (Ag/AgCl) as the reference electrode. All potentials given in the text are referred to this electrode. The electrooxidation of ABA was performed on gold wire electrodes or on the ITO glass electrodes (indium tin oxide coated glass) by potential cycles from –0.2 V to 1.2V *vs.* Ag/AgCl. The typical scan rate was equal to 20 mV/s for gold and 10 mV/s for ITO electrodes. The electrooxidation products obtained on ITO were studied by *in situ* UV-VIS absorption spectra at constant potential, as well as by recording the absorbance change during cyclic potential sweep (10 mV/s) at the constant wavelength. The samples for the IR measurements were electrodeposited on the Pt sheet. Subsequently, three potential cycles from –0.1 to +0.8 V and back to –0.1 V were carried out. The samples were rinsed with water, dried and detached from the electrode. IR spectra were recorded in KBr pellets using Shimadzu FTIR 8400 spectrometer. Electrochemical part of experiments was maintained by the AUTOLAB system (Eco Chemie, The Netherlands). *In situ* VIS absorption spectra were recorded by the Lambda 12 Perkin Elmer spectrometer. The monomer ABA and acids (Fluka) were used as obtained without further purification.

RESULTS AND DISCUSSION

Cyclic voltammograms of ABA in 2M H_2SO_4. Typical voltammograms obtained during the electrooxidation of ABA in the 2M H_2SO_4 solution are shown in Figure 1. On the first positive sweep the peak (A) corresponding to the oxidation of ABA is observed at 1.05 V. Single redox couple corresponding to ABA electrooxidation products occurs in initial electrooxidation cycles. In the few initial cycles both A and B/B′ currents diminish, as indicated by arrows in Figure 1, suggesting that the product of ABA electrooxidation is not very electroactive and it is blocking the electrode surface. During further cycling, the B/B′ pair increases in a way characteristic for growth of the electroactive film. Further new redox pairs appear: C/C′ and D/D′ in Fig. 1. Such delayed growth of the electroactive layer was observed during the electrooxidation of *o*-aminophenol (OAP) [14,15]. The main product of the OAP electrooxidation was the cyclic dimer – 3-aminophenoxazone, which underwent further oxidation and polymerization. The obtained polymer had the ladder – phenooxazine type structure. By analogy, in our case the cyclic dimers/oligomers might be formed during the first oxidation–reduction cycles in the ABA solution.

Fig. 2 shows cyclic voltamperometric responses of the layers obtained in 10, 15, 20 and 25 ABA electrooxidation cycles recorded in the monomer free 2M H_2SO_4 solution. As illustrated in Fig. 2, two or three redox pairs are discernable depending on the layer thickness. Poly-OAP showed the single redox pair in similar experimental conditions [14,15].

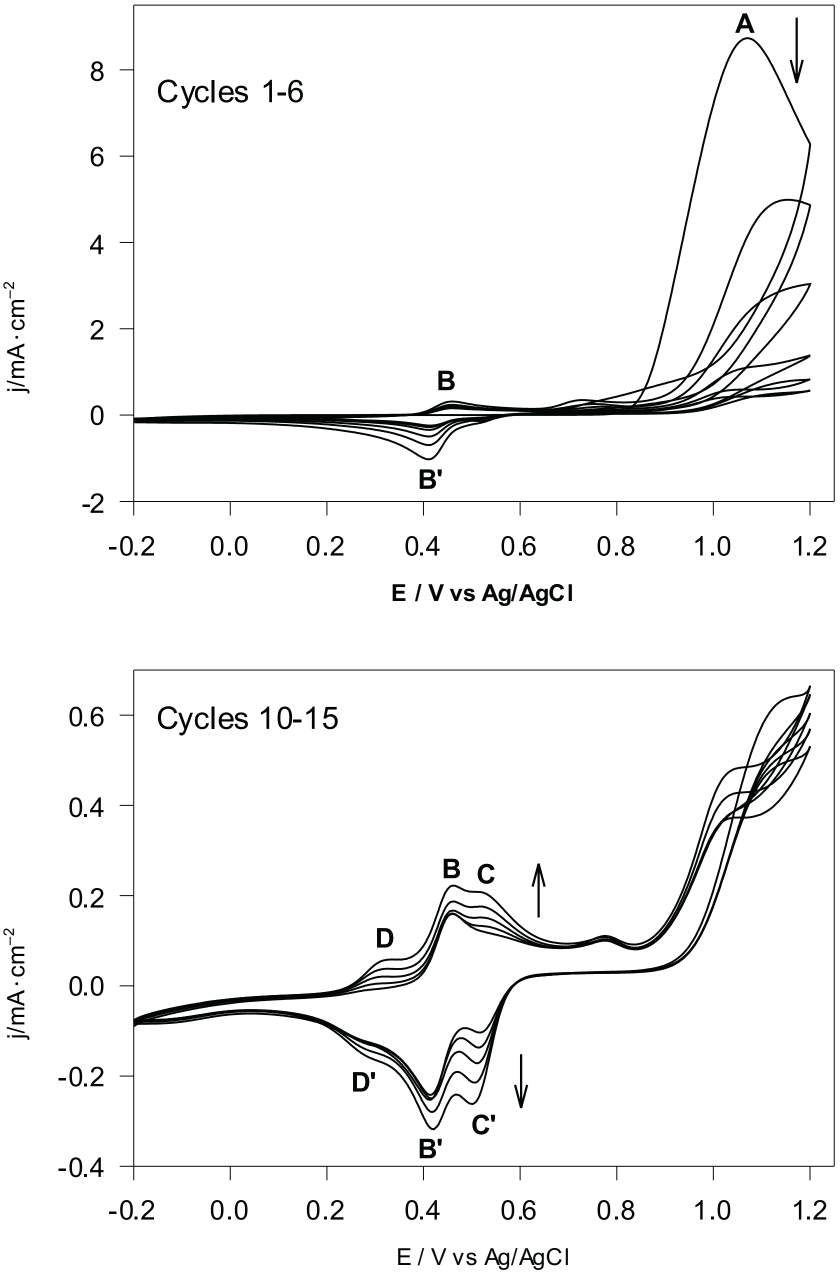

Figure 1. Cyclic voltammograms recorded during the ABA electrooxidation at the gold electrode in 2 M H_2SO_4; sweep rate 20 mV/s; arrows indicate current changes in subsequent cycles.

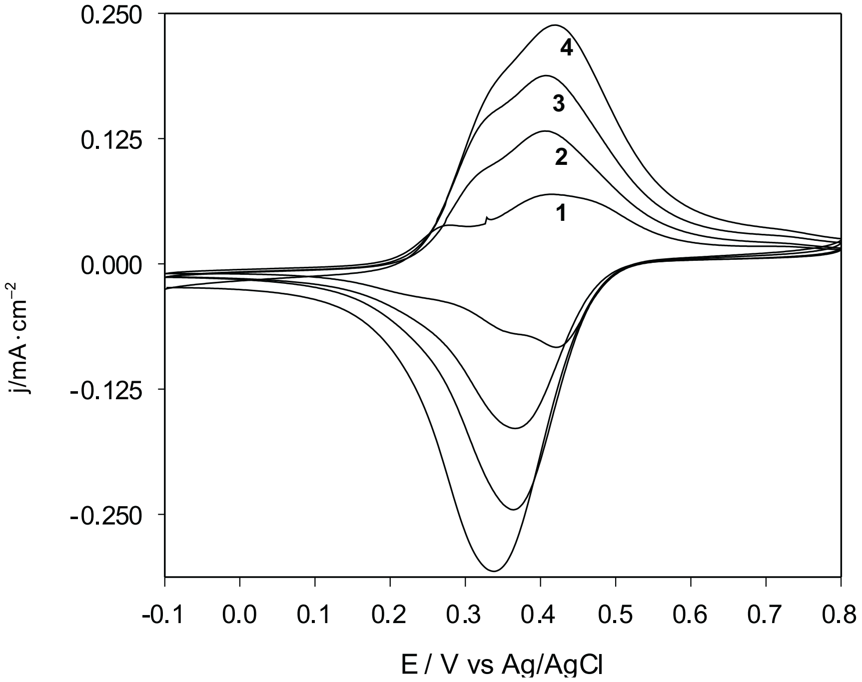

Figure 2. Cyclic voltammograms in the monomer free solution. Layers electrodeposited in: 1) 10; 2) 15; 3) 20 and 4) 25 cycles. Sweep rate = 20 mV/s.

Infrared spectra. In order to verify presence of phenoxazine structures and find possible differences in chemical composition of thin and thick electrodeposited layers infrared spectra were studied. Fig. 3 presents spectra of the layers deposited in 10, 15, 20, 25 cycles, together with the spectrum of the monomer. None of these spectra show bands characteristic for phenazine ring [15], thus presence of cyclic dimers or polymeric ladder structures among the electrooxidation products can be excluded. As visible in Fig. 3, spectra of thin layers reveal a strong band at 1223 cm^{-1}, which has not been observed in the monomer spectrum. Bands, having similar position and intensity are characteristic for aromatic ethers. Simultaneously, the strong band at 1007 cm^{-1} band characteristic for the monomer CH_2OH group is not observed in spectra of thin electrodeposited layers, corroborating the suggestion that the ether bonds might be formed during the ABA electrooxidation. Furthermore, the band observed at 595 cm^{-1} in thin layer spectra originates probably from the C–O–C out-of-plane deformation.

The strong band at 748 cm^{-1} observed solely in the monomer spectrum corresponds to benzene out-of-plane mode. The position of this mode depends on the ring substitution. In the spectra of thin electrodeposited layers this mode is replaced by a broad band at 850 cm^{-1}, suggesting that the substitution of benzene ring is changed from 1, 2 to 1, 2, 4 or 1, 2, 3. Consequently, the thin electrodeposited layers contain oligomeric benzyl ether structures depicted in Fig. 4: **1** and **2**.

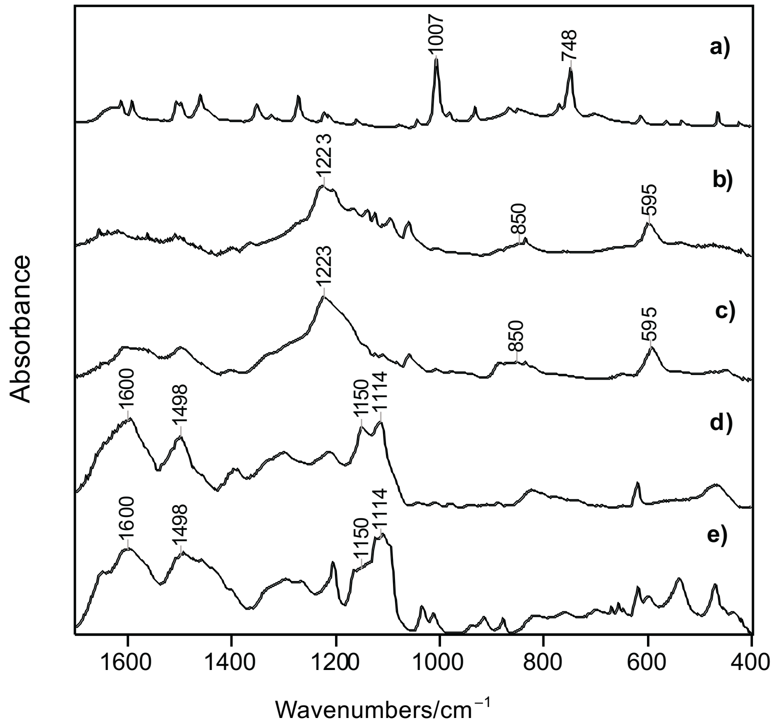

Figure 3. Infrared spectra of a) ABA and ABA electrooxidation products obtained by b) 10; c) 15; d) 20 and e) 25 cycles.

Spectra shown in Fig. 3 reveal also that further electrooxidation changes the structure of obtained layers. In spectra of layers deposited in 20 and 25 cycles the ether band at 1223 cm^{-1} is less intense in comparison to neighbouring bands. The bands at: 1600, 1498, 1150 and 1114 cm^{-1} are dominating the thick layers spectra. Their frequencies coincide with bands characteristic for the benzenoid PANI rings [19,20]. In result, it may be concluded that the PANI-like polymer (structure **3** in Fig. 4) deposits when the electropolymerization is carried out by more than 15 cycles.

UV/VIS absorption spectra of thin and thick PABA layers. The electrooxidation of ABA has been studied also on ITO glass electrodes. Typical cyclic voltammetry curves closely resemble those obtained on gold electrodes (Fig. 1) and therefore they are not shown. Figure 5 shows *in situ* UV/VIS spectra obtained for the layer deposited during ten potential cycles. The *in situ* UV/VIS absorption spectra of such layer show a single absorption band with a maximum at 530 nm with a long VIS-tail. Upon changing the electrode potential the 530 nm band changes the intensity, indicating electrochromic properties of the layer, although the polaron and bipolaron absorptions typical for PANI are not observed. The *in situ* UV/VIS spectra confirm thus that the thin electrodeposited layers do not contain the PANI like polymer. The 530 nm band correspond thus to the oligomeric structures **1** and **2** proposed in Fig. 4.

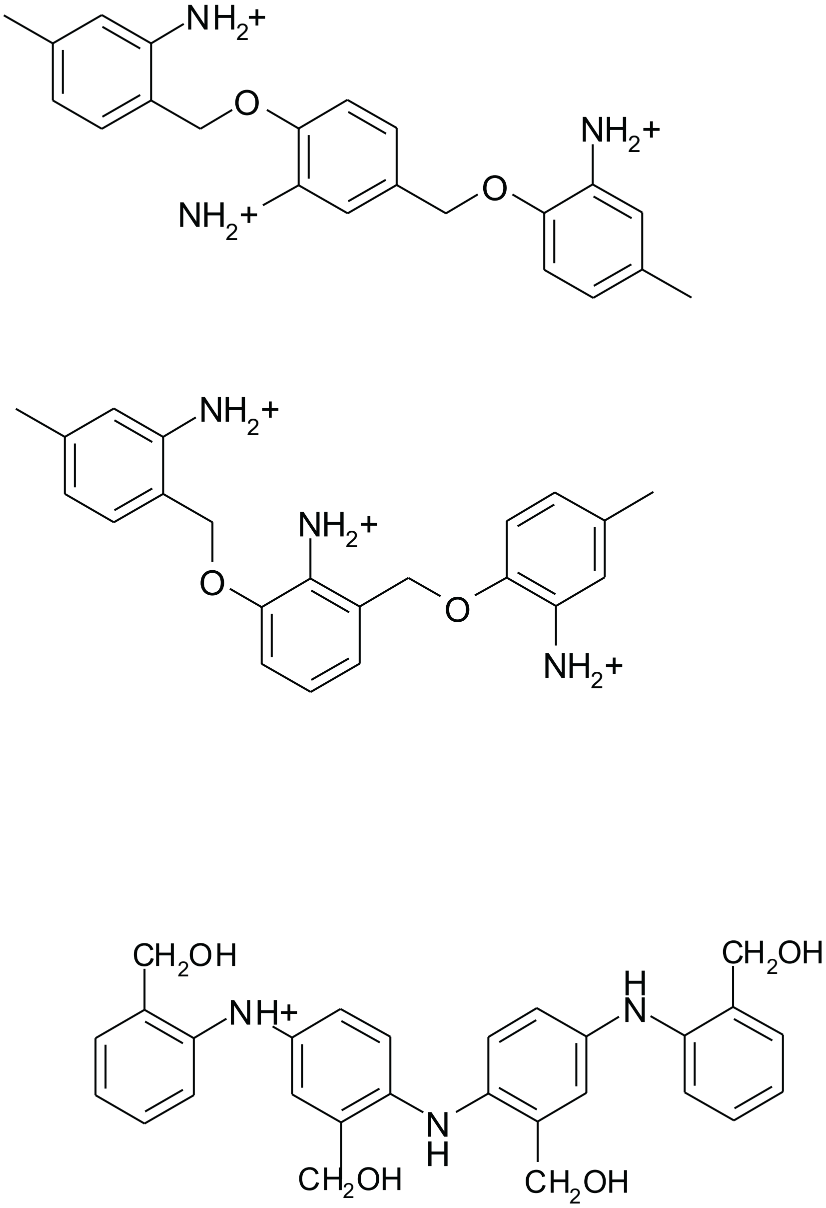

Figure 4. Proposed structures of ABA electrooxidation products. **1** and **2** – structures obtained during initial electrooxidation cycles; **3** – structure formed after more than 15 cycles.

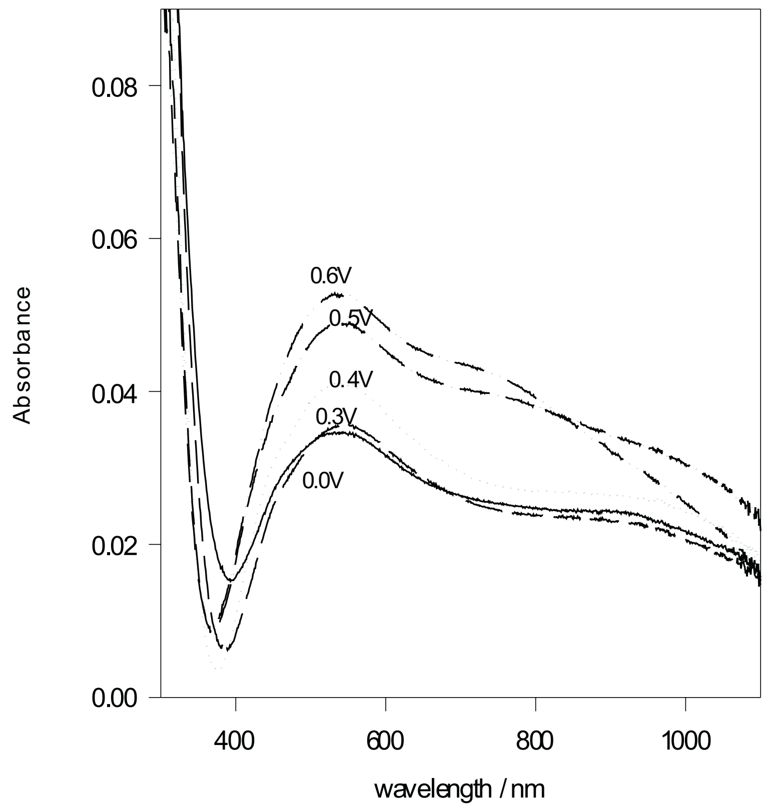

Figure 5. *In situ* UV/VIS absorption spectra of the layer obtained by 10 ABA electrooxidation cycles recorded at various potentials: —— 0.0 V; — — +0.3 V; · · · · · · · · +0.4 V; — • — +0.5 V; — · · — +0.6 V.

The dependence of the UV/VIS absorption spectra on the electrode potential differs for thicker PABA layers. Figure 6 shows spectra of the layer obtained by twenty oxidation–reduction cycles. The clear band at 440 nm develops due to changing the electrode potential from 0.0 V to 0.45 V. By analogy with PANI [21,22] the increase of this band can be attributed to the polaron formation. Further oxidation of the layer cause diminishing of the 440 nm band and growth of the new band located at 720 nm, which corresponds to bipolaron states. The spectral characteristics of the thick layers stays in agreement with the presence of PANI – like polymer (structure **3** in Fig. 4) in the thick electrodeposited layers.

dA/dt *versus* potential plots. To compare the observed spectra with cyclic voltammograms changes of absorbance *versus* potential were studied at fixed wavelengths. Three wavelengths were chosen: 440 nm corresponding to the polaron absorption band, 720 nm falling in the bipolaron band and 530 nm corresponding to the oligomeric benzyl ether species. Values of absorbance were differentiated *versus* time in order to obtain plots directly comparable with cyclic voltammograms. Typical

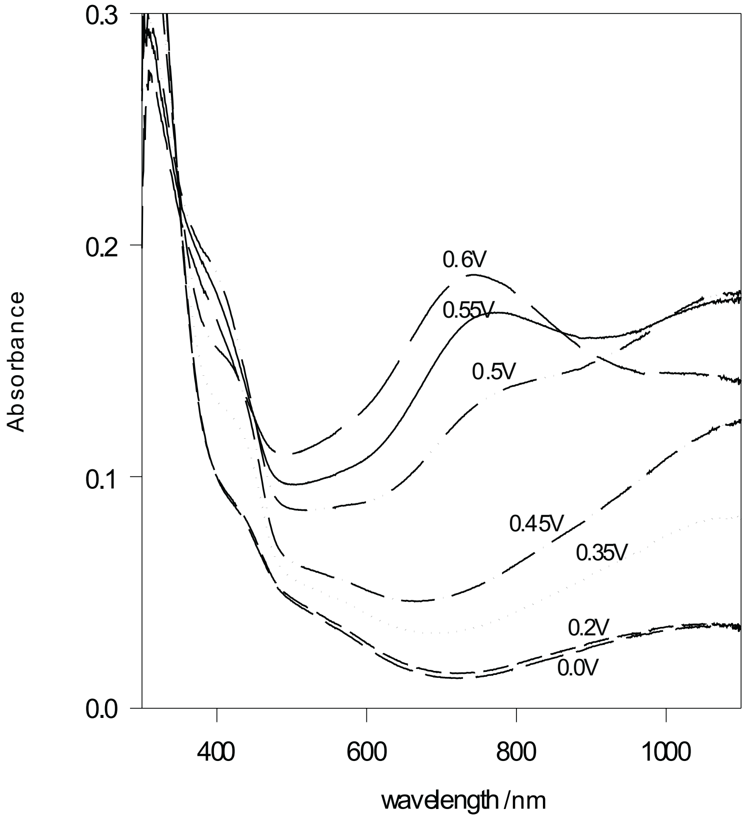

Figure 6. In situ UV/VIS absorption spectra of the layer obtained by 20 ABA electrooxidation cycles recorded at various potentials: ——— 0.0 V; ———— +0.2 V; ······· +0.35 V; — • — +0.45 V; — ·· — +0.5 V; ——— +0.55 V; —— +0.6 V.

results obtained for the layer deposited by 20 cycles are presented in Figure 7. The redox couples are marked consistently with Fig. 1.

As visible in Fig. 7, the maximum of the dA/dt plot for 440 nm match the first oxidation peak (D) on cyclic voltammogram. Consequently, the D/D′ redox couple corresponds to the first redox reaction of the PANI type polymer.

The 720 nm and 530 nm plots correspond to bipolaronic and oligomeric species respectively. These plots show maxima in the similar potential range. Therefore, their contributions to the cyclic voltammogram are difficult to discern. Although, shapes of 530 nm and 720 nm plots are clearly different, indicating that thick layer contain the two products of ABA electrooxidation.

Influence of the acid concentration on the ABA electropolymerization. The effect of anions and the influence of acid concentration on electrooxidation of aniline and substituted anilines have been demonstrated by many authors [23–28]. To investigate these effects on PABA formation we have studied the electrooxidation of the

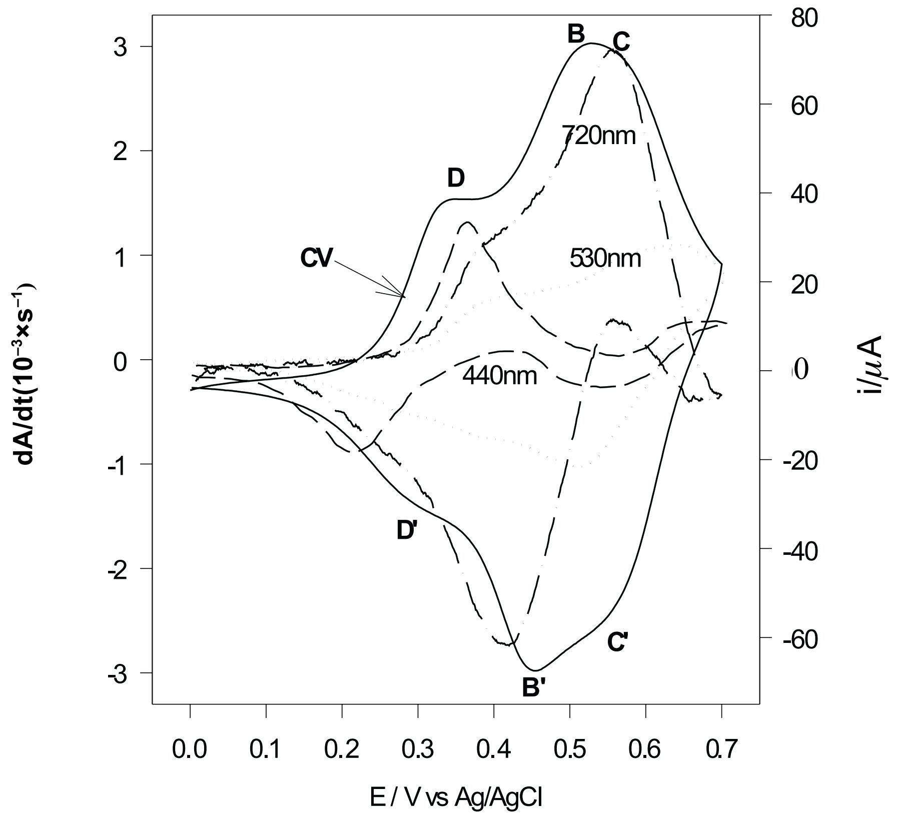

Figure 7. dA/dt plots and cyclic voltammogram of layer obtained by 20 ABA electrooxidation cycles; sweep rate = 10 m V/s. ——— cyclic voltammogram; — — dA/dt plot for λ = 440 nm; — · — dA/dt plot for λ = 720 nm; · · · · · dA/dt plot for λ = 530 nm.

ABA in H_2SO_4 or $HClO_4$ environment. It has been demonstrated that these two acids have distinct influence on electropolymerisation of PANI and substituted polyanilines. The monomer concentration was equal to 0.1 M and the acid concentrations were varied from 0.2 to 2 M for the H_2SO_4 and from 0.4 to 4 M in case of $HClO_4$.

The potentials of the monomer oxidation in the first oxidation-reduction cycle are similar in all studied solutions. Further voltammetric responses develop depending on the acid concentration. Figure 8 shows typical cyclic voltammograms obtained in 0.2 M sulphuric acid. As may be seen in Fig. 8, the shape of cyclic voltammograms does not change anymore since 8th cycle. The obtained electroactive layer is characterized by the single oxidation-reduction pair. Consequently, it may be concluded that such layer does not contain the structure **3** (Fig. 4) and possibly oligomers containing benzylether units deposit on the electrode surface. Similarly, in case of the diluted perchloric acid solution the ABA electrooxidation yields the electroactive layer, characterized by the single redox pair.

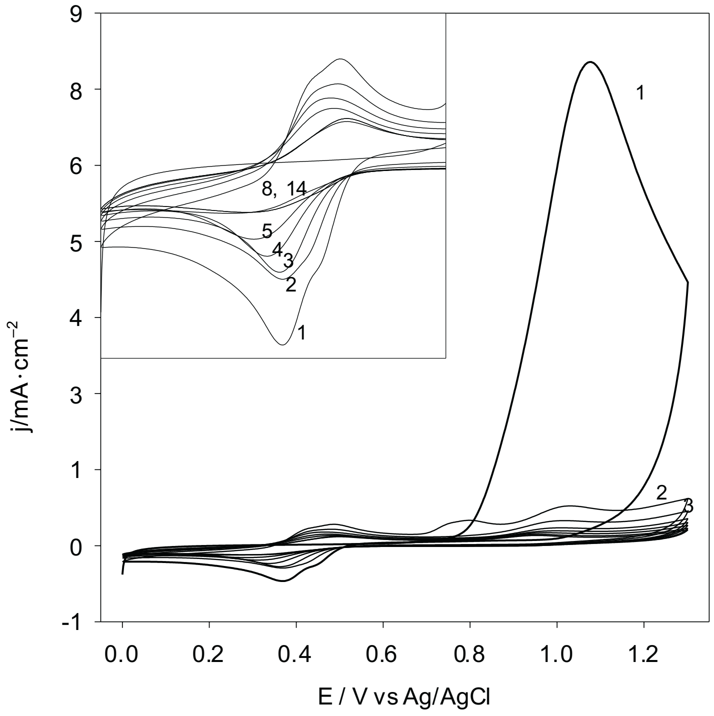

Figure 8. Cyclic voltammograms obtained during the ABA electrooxidation at the gold electrode in 0.2 M H_2SO_4; sweep rate 20 mV/s; numbers of cycles indicated.

For both sulphuric and perchloric acids the increase of the acid concentration changes the course of the ABA electrooxidation. Cyclic voltammograms develop similarly to those presented in Fig. 1 and the obtained layers are characterized by three redox pairs. The effect of the acid concentration on cyclic voltammograms is visible in Fig. 9, where cyclic voltammograms of PABA layers obtained at various H_2SO_4 concentrations are collected. The presented cyclic voltammograms have been recorded for the layers obtained in 15 cycles. Analogous voltammograms for $HClO_4$ are shown in Figure 10. By comparison of Figures 9 and 10 it may be concluded that the kind of acid influences the differences ΔE between peak potentials of the first and the third redox pair. Similar anion influence on cyclic voltammograms has been observed for poly-dimethoxyaniline [28]. Furthermore, the ratio of peak currents of the outer to the middle redox pairs suggests that formation of the PANI analogue polymer is facilitated in presence of $HClO_4$.

The currents obtained for layers prepared in 4 M acid are significantly lower than those obtained for lower acid concentrations as visible in Fig. 10, though the studied layers have been obtained in the same number of cycles. The charge passing during the anodic potential sweep in the monomer free solution (Q_+) can be used as an estimation of the amount of the electrodeposited species. Fig. 11 shows the dependence of Q_+ on the acid concentration for layers obtained in 15 cycles. Fig. 11 indicates that

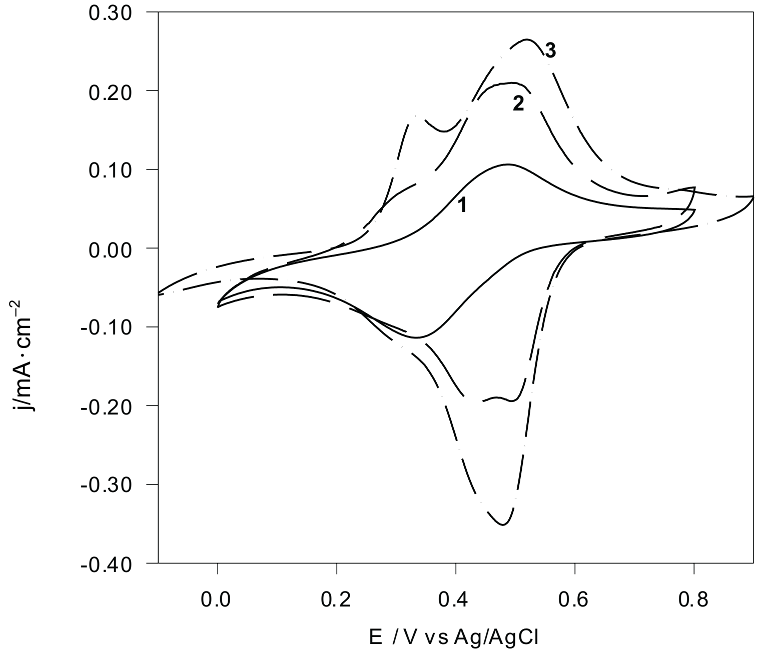

Figure 9. Cyclic voltammograms of ABA electrooxidation products recorded in monomer free solutions. PABA layers were obtained in 1) 0.2 M H_2SO_4; 2) 1 M H_2SO_4; 3) 2 M H_2SO_4.

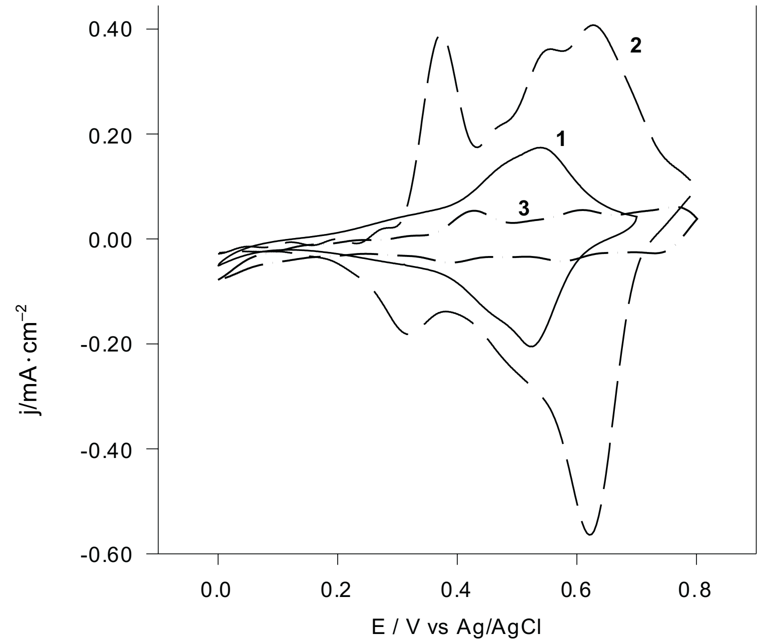

Figure 10. Cyclic voltammograms of ABA electrooxidation products recorded in monomer free solutions. PABA layers were obtained in 1) 0.4 M $HClO_4$; 2) 2 M $HClO_4$; 3) 4 M $HClO_4$.

the increase of the acid concentration from 0.2 up to 1–2 M results in increased amount of electrodeposited species, while further increase of the acid concentration causes the opposite effect. By analogy with PANI [23], we suppose that the electropolymerization of ABA requires strongly acidic conditions and accordingly the higher Q_+ values are expected for high acid concentration. The low electropolymerization efficiency for 3 and 4 M acid can be attributed to the increased solubility of intermediate polymerization products in high acid concentration, preventing the precipitation and further oxidation of oligomers. Another hindrance for the electropolymerization in 3 and 4 M acid is possible hydrolysis of oligomers in such media [29].

CONCLUSIONS

Two kinds of electroactive and electrochromic products are formed during the electropolymerization of ABA. These products have been identified by infrared and UV/VIS absorption spectra. The oligomers containing benzylether structures cover the electrode surface in initial electrodeposition cycles. During further ABA electrooxidation the polymer similar to PANI is formed. The relative amounts of these two products depend on the concentration and on the kind of the acid present in the electropolymerization bath.

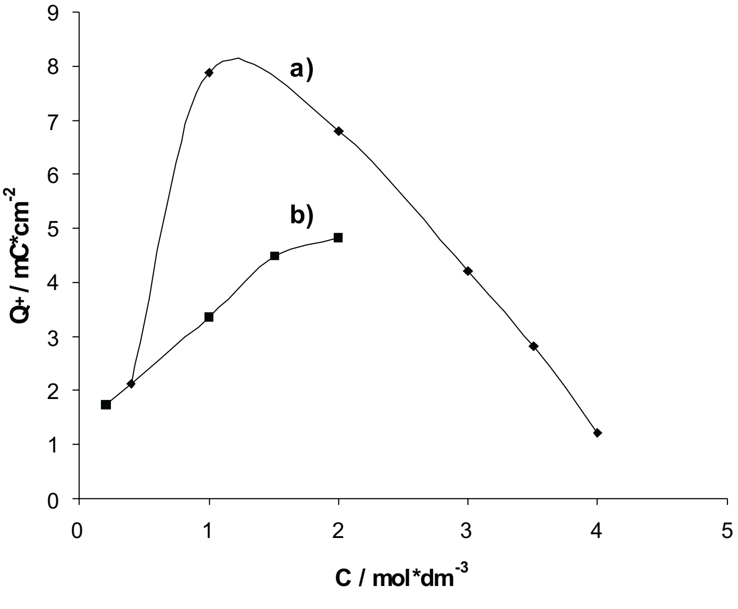

Figure 11. Dependence of the charge passing during the anodic potential sweep in the monomer free solution (Q_+) on the acid concentration (C) for: a) perchloric and b) sulphuric acid.

REFERENCES

1. Wei Y., Focke W.W., Wnek G.E., Ray A. and MacDiarmid A.G., *J. Phys. Chem.*, **93**, 495 (1989).
2. Genies E.M. and Noel P., *J. Electroanal. Chem.*, **310**, 89 (1991).
3. Lacroix J.C., Garcia P., Audiére J.P., Clément R. and Kahn O., *Synth. Met.*, **44**, 117 (1991).
4. Cattarin S., Doubova L., Mengoli G. and Zotti G., *Electrochim. Acta*, **33**, 1077 (1988).
5. Zhang A.Q., Cui C.Q. and Lee J.Y., *J. Electroanal. Chem.*, **413**, 143 (1996).
6. Rivas B.L., Sanchez C.O., Bernede J.-C. and Mollinie P., *Polymer Bulletin*, **49**, 257 (2002).
7. Gazotti W.A. Jr., Faez R. and De Paoli M.A., *J. Electroanal. Chem.*, **415**, 107 (1996).
8. Penneau J.F., Łapkowski M. and Genies E.M., *New. J. Chem.*, **13**, 449 (1989).
9. Goncalves D., Matosso L.H.C. and Bulhoes L.O.S., *Electrochim. Acta*, **39**, 2271 (1994).
10. Zotti G., Comisso N., D'Aprano G. and Leclerc M., *Adv. Mater.*, **47**, 49 (1992).
11. Chiba K., Ohsaka T., Ohnuki Y. and Oyama N., *J. Electroanal. Chem.*, **219**, 117 (1987).
12. Tucceri R.I., Barbero C., Silber J.J., Sereno L. and Posadas D., *Electrochim. Acta*, **42**, 919 (1997).
13. Cintra E.P., Cordoba de Torresi S.I., Errien N. and Louarn G., *Macromolecules*, **36**, 2079 (2003).
14. Jackowska K., Bukowska J. and Kudelski A., *Polish J. Chem.*, **68**, 141 (1994).
15. Barbero C., Silber J.J. and Sereno L., *J. Electroanal. Chem.*, **263**, 333 (1989).
16. Goncalves D., Faria R.C., Yonashiro M. and Bulhoes L.O.S., *J. Electroanal. Chem.*, **487**, 90 (2000).
17. Rivas B.L. and Sanchez C.O., *J. Appl. Polym. Sci.*, **82**, 330 (2001).
18. Widera J., Grochala W., Jackowska. K. and Bukowska J., *Synth. Met.*, **89**, 29 (1997).
19. Ping Z., Nauer G.E., Neugebauer H., Theiner J. and Neckel A., *Electrochim. Acta*, **42**, 1693 (1997).
20. Trchova M., Stjeskal J. and Prokes J., *Synth. Met.*, **101**, 840 (1999).
21. Genies E.M. and Łapkowski M., *J. Electroanal. Chem.*, **220**, 67 (1987).
22. Stilwell D.E. and Su-Moon Park, *J. Electrochem. Soc.*, **135**, 427 (1989).
23. Zotti G., Catarin S. and Comisso N., *J. Electroanal. Chem.*, **239**, 387 (1988).
24. Inzelt G. and Horanyi G., *Electrochim. Acta*, **35**, 27 (1990).
25. Kalaji M., Nyholm L. and Peter L.M., *J. Electroanal. Chem.*, **313**, 271 (1991).
26. Tang H., Kitani A. and Shiotani M., *Electrochim. Acta*, **41,** 1561 (1996).
27. Widera J., Palys B., Bukowska J. and Jackowska K., *Synth. Met.*, **94**, 265 (1998).
28. Palys B., Kudelski A., Stankiewicz A. and Jackowska K., *Synth. Met.*, **108**, 111 (2000).
29. Kobayashi T., Yoneyama H. and Tamura H., *J. Electroanal. Chem*., **177**, 293 (1984).